5

Evaluation of RGD-targeted Albumin Carriers for Specific Delivery of Auristatin E to Tumor Blood Vessels

Kai Temming[1,2], Damon L. Meyer[3], Roger Zabinski[3], Eli C. F. Dijkers[4], Klaas Poelstra[1], Grietje Molema[5], Robbert J. Kok[1,6]

[1] Department of Pharmacokinetics and Drug Delivery, Groningen University Institute for Drug Exploration (GUIDE), Groningen, The Netherlands
[2] KREATECH Biotechnology B.V. Amsterdam, The Netherlands
[3] SEATTLE GENETICS, Bothell, WA, USA
[4] Department of Nuclear Medicine and Molecular Imaging, University Medical Center Groningen, Groningen, The Netherlands.
[5] Department of Pathology and Laboratory Medicine, Medical Biology Section, University Medical Center Groningen, University of Groningen, The Netherlands
[5] Department of Pharmaceutics, Utrecht Institute for Pharmaceutical Sciences (UIPS), Utrecht, The Netherlands

Bioconjugate Chemistry (2006), 17, 1385 – 1394.

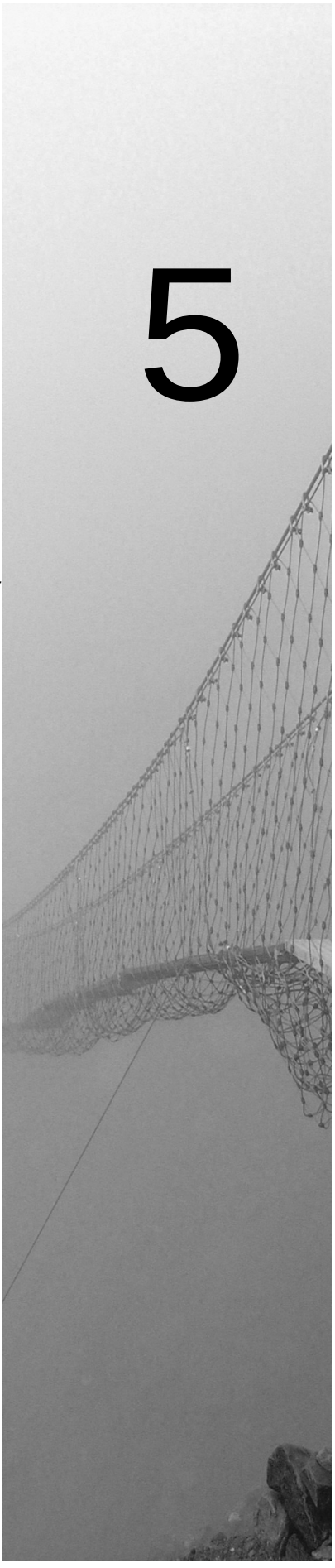

Abstract

Induction of apoptosis in endothelial cells is considered an attractive strategy to therapeutically interfere with a solid tumor's blood supply. In the present paper, we constructed cytotoxic conjugates that specifically target angiogenic endothelial cells thus preventing typical side effects of apoptosis inducing drugs. For this purpose, we conjugated the potent antimitotic agent monomethyl-auristatin-E (MMAE) via a lysosomal cleavable linker to human serum albumin (HSA), and further equipped this drug-albumin conjugate with cyclic c(RGDfK) peptides for multivalent interaction with $\alpha_v\beta_3$-integrin. The RGD-peptides were conjugated via either an extended polyethylene-glycol linker or a short alkyl linker. The resulting drug-targeting conjugates RGDPEG-MMAE-HSA and RGD-MMAE-HSA demonstrated high binding affinity and specificity for $\alpha_v\beta_3$-integrin expressing human umbilical vein endothelial cells (HUVEC). Both types of conjugates were internalized by endothelial cells, and killed the target cells at low nM concentrations. Furthermore, we observed RGD-dependent binding of the conjugates to C26 carcinoma. Upon i.v. administration to C26-tumor bearing mice, both drug-targeting conjugates displayed excellent tumor homing properties. Our results demonstrate that RGD-modified albumins are suitable carriers for cell selective intracellular delivery of cytotoxic compounds, and further studies will be conducted to assess the antivascular and tumor inhibitory potential of RGDPEG-MMAE-HSA and RGD-MMAE-HSA.

Introduction

Excessive angiogenesis, the formation of new blood vessel out of pre-existing capillaries, is a prominent feature during the pathogenesis of cancer. Solid tumors rely on angiogenesis to guarantee a continuous supply of oxygen and nutrients. Vascular directed therapies are therefore extensively investigated for combating cancer [1]. Induction of apoptosis in endothelial cells is one way to destroy tumor vessels. However, most cytotoxic compounds are neither selective for endothelial cells in general nor for angiogenic endothelial cells. As a consequence, they produce severe side effects limiting their applicability in cancer therapy. We propose targeting of the antimitotic agent monomethyl auristatin E (MMAE) to angiogenic blood vessels in tumor tissue. MMAE, a synthetic analog of the natural product dolastatin 10, is a potent inhibitor of tubulin polymerization in dividing cells [2, 3]. Previously, MMAE has been conjugated via a valine-citrulline linker to monoclonal antibodies (mAb) for drug targeting purposes [3-6]. The valine-citrulline linker is highly stable in serum but is cleaved by lysosomal enzymes like cathepsin B after internalization of the conjugate by target cells [7-9]. We now present a novel type of MMAE conjugate, in which the drug is bound via the valine-citrulline linker to human serum albumin (HSA). HSA is readily available in gram amounts, and can serve as a natural and therefore biocompatible and biodegradable carrier with a lower polydispersity than any artificial polymeric carrier. Selectivity for angiogenic endothelial cells is introduced into the albumin backbone by conjugation of multiple cyclic RGD-peptides, which bind to $\alpha_v\beta_3$-integrin [10]. We applied either a short alkyl linker to introduce a maximum of RGD-peptide or an extended polyethylene glycol linker, to infer an increased circulation time and shielding of the modified albumin from the immune system. The $\alpha_v\beta_3$-integrin target receptor is expressed in high amounts on angiogenic endothelium but expression is minimal on quiescent endothelial cells and highly limited in other healthy tissues. The restricted expression profile and the good accessibility of endothelial cells make it an ideal target for drug delivery purpose [11]. We have previously described that RGD-equipped carriers bind with high avidity to proliferating endothelial cells, and that they are internalized and lysosomal degraded [12-14].

In the present study, we first describe the synthesis and characterization of the two types of RGD-equipped MMAE-albumin conjugates. Second, we report on the binding, uptake and cell killing properties of the conjugates, and we compared the tumor vasculature homing potential in C26 tumor bearing mice.

Materials and Methods

Synthesis and Purification of MMAE-HSA

HSA (Sanquin, Amsterdam, The Netherlands) was thiolated with 2-iminothiolane (2-IT) at pH 8, 37 ºC. Thiolation was monitored by DTNB of PD10-purified analytical samples. When the desired thiolation level was reached (4.1 SH/Albumin), the modified albumin was purified over a G25 gel filtration desalting column. The thiol/albumin mole ratio was determined by measuring the thiol concentration with Ellman's assay and the albumin concentration by UV absorbance at 280 nm. Thiolated albumin was treated with a 20% excess (over measured thiols) of MC-val-cit-PAB-MMAE. Ellman's assay was performed on the reaction mixture to ensure complete alkylation. Excess maleimide-drug-linker was quenched, and removed with solid-phase resin-bound-DTT (BioVectra cat. #3505), and the product was purified by gel filtration chromatography.

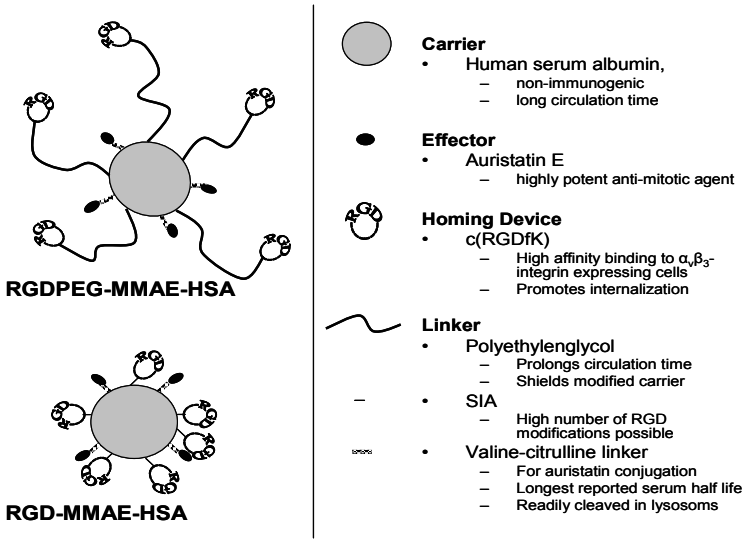

Figure 1. Schematic representation of RGD-equipped MMAE-albumin conjugates

Characterization of MMAE-HSA

The concentration of the MMAE-HSA conjugates was measured using the BCA assay kit from Pierce. The MMAE-HSA conjugate was analyzed by size exclusion chromatography for percentage of monomer using a Tosoh Bioscience TSKgel G3000SW (7.8 cm x 30 cm, 5 µm) size exclusion chromatography (SEC) column. The conjugates were more than 91% monomer. To check for residual drug-linker, a sample of conjugate was treated with MeOH and separated in a microconcentrator to precipitate the protein, and the supernatant was analyzed by reverse phase (RP) HPLC (Synergi C12 column with a linear gradient from 5 mM ammonium phosphate, pH 7, to 100% acetonitrile). No free drug-linker was detectable, compared to spiked controls and a standard curve with a quantitation limit of <0.5% of bound drug. The MMAE-HSA conjugates were tested for endotoxin contaminant using BioWhitaker-Cambrex LAL QCL-1000 kit. Endotoxin was below the limit of detection (~0.2 EU/mg).

The drug to HSA ratio was estimated by treating 300 µg of conjugate with Cathepsin B to release free MMAE from the mc-val-cit-PAB linker. The protein was removed by precipitation with TCA/MeOH, heated at 37 °C for 10 minutes, and centrifuged at high speed to pellet. The released drug in the supernatant was analyzed by RP-HPLC as described above for drug-linker, and quantitated by comparison to a standard curve. The drug/albumin values agreed closely (± 5 %) with the thiol/albumin ratios determined prior to conjugation. A change in the OD250/OD280 ratio commensurate with the conjugation of PAB-containing moieties qualitatively corroborated the measured drug load. Thereafter MMAE-HSA was subjected to MALDI-TOF analysis. HSA and MMAE-HSA were dissolved in 50:50:0.1 methanol : water : acetic acid at a concentration of 1 mg/mL. 1 µL was mixed with 1 µL of matrix (20 mg/mL sinapinic acid in 60:40:0.1 water:acetonitrile:trifluoroacetic acid), transferred onto a stainless steel sample holder, and dried before being introduced into a Voyager-DE PRO workstation (Applied Biosystems). Mass spectra

were obtained by averaging the signals from 100 laser shots. Correction of data was performed using BSA as a control. Average molecular weights received by MALDI-TOF analysis were used to calculate differences in mass of HSA to MMAE-HSA.

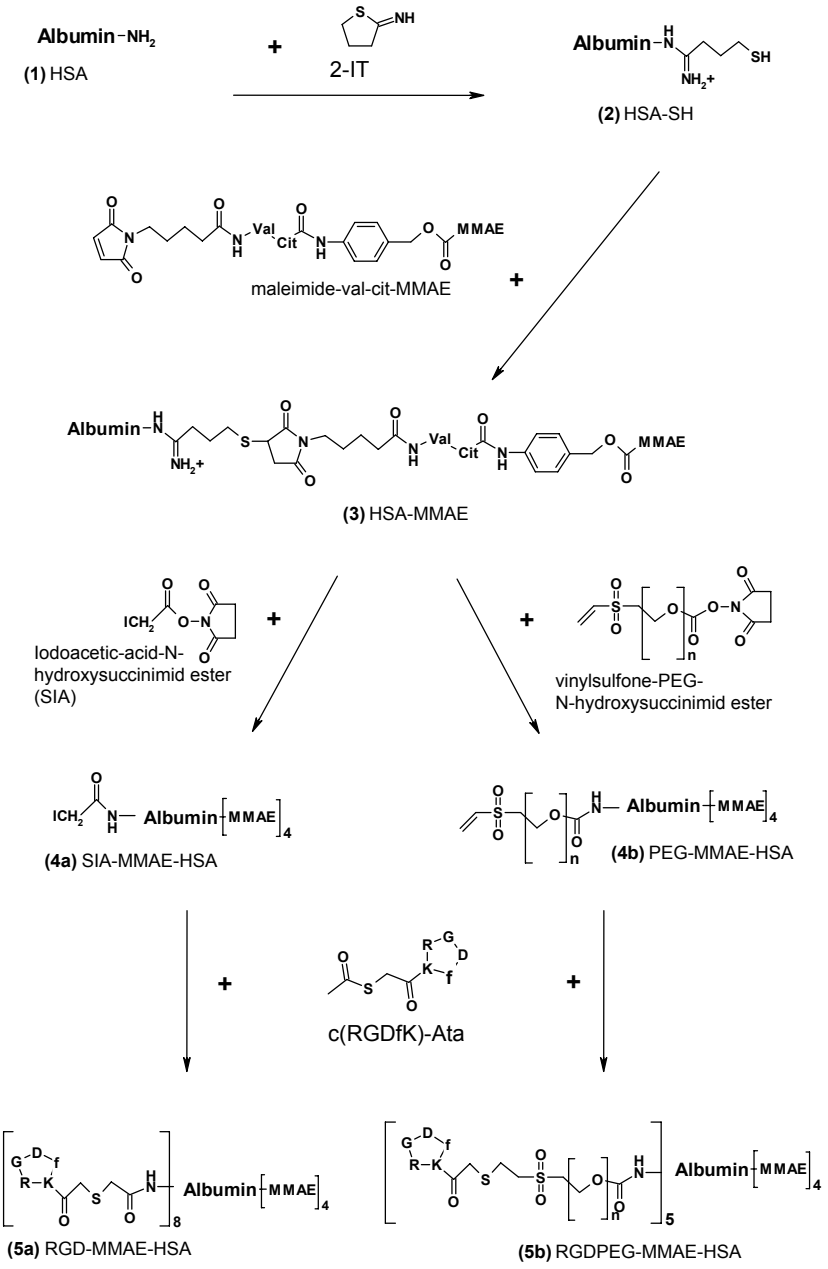

Figure 2. Reaction scheme for the synthesis of RGDPEG-MMAE-HSA and RGD-MMAE-HSA.

Synthesis of RGDPEG-MMAE-HSA

MMAE-HSA (59.1 nmol) dissolved in PBS was incubated with a 50-fold molar excess of vinylsulfone-polyethyleneglycol-N-hydroxysuccinimide ester (VNS-PEG-NHS; Nektar, Alabama, USA; 20 mg/mL in water, 2.96 µmol), which was added dropwise. The mixture was protected from light with aluminum foil, and incubated for 1h at room temperature while gently shaking on a spiramix. Meanwhile, the RGD-peptide c(RGDf(ε-S-acetylthioacetyl)K) (Ansynth Service, Roosendaal, The Netherlands) was dissolved at 10 mg/mL in a 1:4 acetonitrile/water mixture. The peptide (3.25 µmol) was added dropwise to the reaction mixture at a peptide to protein molar ratio of 55:1, after which hydroxylamine was added to a final concentration of 50 mM. Reaction was carried out over night at room temperature while protected from light. Remaining VNS groups were quenched by addition of cysteine (3.25 µmol; 55-fold molar excess over the amount of HSA), after which the product was dialyzed against PBS, and finally purified by SEC using a Superdex200 column on an Äkta System (GE Healthcare, Uppsala, Sweden). The final product RGDPEG-MMAE-HSA was stored at -20 °C. A control conjugate RADPEG-MMAE-HSA was prepared according to the same protocol with the control peptide c(RADf(ε-S-acetylthioacetyl)K).

Synthesis of RGD-MMAE-HSA

MMAE-HSA (59.1 nmol) dissolved in PBS was incubated with a 22-fold molar excess of iodoacetic acid N-hydroxysuccinimide ester (SIA-linker; Sigma, MO, USA; 10 mg/mL in DMF, 1.3 µmol), which was added dropwise. The mixture was protected from light with aluminum foil, and incubated for 1 h at room temperature while gently shaking on a spiramix. RGD-peptide (1.48 µmol) was added in a mole:mole ratio of 25:1 followed by hydroxylamine addition as described above. Reaction was carried out within six hours at room temperature while protected from light. Products are purified by dialyzing three times against PBS using Slide-A-Lyzer dialysis cassettes (Pierce, MWCO 10 kDa). The final products RGD-MMAE-HSA and the control conjugate RAD-MMAE-HSA were stored at -20 °C.

Characterization of RGDPEG-MMAE-HSA and RGD-MMAE-HSA

Protein content of synthesis products was estimated by BCA protein assay kit (Pierce). Both the intermediate and final products were subjected to analytical SEC to reveal increase in size, purity, and grade of aggregation. SDS-PAGE (12 %, Ready Gel; Bio-Rad, Veenendaal, The Netherlands) and Western blotting were performed to corroborate covalent binding of the RGD-peptide. Duplicate gels were either stained for protein (Coomassie Brilliant Blue staining) or blotted on a PVDF membrane (Roche, Mannheim, Germany). The membrane was blocked with BSA, and subsequently incubated with an in-house prepared rabbit anti-RGD antiserum [12]. The signal was amplified with a polyclonal goat anti rabbit IgG conjugated with horse radish peroxidase (GARPO, DAKO). Peroxidase was visualized by incubation with 3-amino-9-ethyl-carbazole (AEC, Sigma). The amount of RGDPEG and RGD bound per HSA was determined by MALDI-TOF analysis, as explained earlier in this section.

Cells

HUVEC were obtained from the UMCG Endothelial Cell Facility. Primary isolates were cultured in 1% gelatin-coated tissue culture flasks (Costar, Cambridge, MA, USA) at 37 °C under 5% CO2 / 95% air. The culture medium, hereafter referred to as EC medium, consisted of RPMI 1640 (BioWittaker, Verviers, Belgium) supplemented with 20% heat inactivated fetal calf serum (Integro, Zaandam, The Netherlands), 2 mM L-glutamine (Invitrogen, Breda, The Netherlands), 5 U/mL heparin (Leo Pharmaceutical Products, Weesp, The Netherlands), 100 U/mL penicillin (Yamanouchi Pharma, Leiderdorp, The Netherlands, 100 µg/mL streptomycin (Radiumfarma-Fisiopharma, Italy), and 50 µg/mL EC growth factor supplement extracted from bovine brain. After attaining confluence, cells were detached from the surface by trypsin EDTA (0.5/0.2 mg/mL in PBS) treatment, and split in 1:3 ratio. Cells were used up to passage four.

C26 mouse carcinoma cells were cultured under the same conditions as described for HUVEC, in DMEM medium (Gibco) containing 10% fetal calf serum.

Endothelial Cell Binding Affinity of RGD-equipped Conjugates

Binding affinity of RGDPEG-MMAE-HSA and RGD-MMAE-HSA to $\alpha_v\beta_3$-integrin expressed on the surface of HUVEC was determined by competitive binding studies using ^{125}I-labeled echistatin as radioligand for $\alpha_v\beta_3$-integrin [15]. Echistatin was radiolabeled using the chloramine T method [16]. On the day of the experiment, ^{125}I-Echistatin was purified using a PD-10 column (GE Healthcare). Confluent monolayers of HUVEC in a 24 well plate (Costar) were incubated with 100,000 cpm ^{125}I-Echistatin in the presence of serial dilutions of the conjugates in binding buffer (50 mM Tris-HCl, pH 7.4, 150 mM NaCl, 1mM $CaCl_2$, 1 mM $MgCl_2$, 1 mM $MnCl_2$ and 1% BSA) at 4 °C for 4 h [13]. Subsequently, the supernatant was harvested, cells were washed three times with binding buffer, and lysed with 1 M NaOH. Radioactivity was counted in a Packard RIASTAR multiwell gamma counter (GMI, Minnesota, USA). Data were analyzed by non-linear regression using the GraphPad Prism program (GraphPad Software Inc).

Binding Specificity of RGD-equipped Conjugates to Endothelial Cells and Tumor Cells

HUVEC were incubated with ^{125}I-radiolabeled RGDPEG-MMAE-HSA and RGD-MMAE-HSA, which had been radiolabeled using the chloramine T method, and purified on the day of the experiment. Radiochemical purity as determined by trichloroacetic acid precipitation was above 96 %, and specific activity was 690 kBq/µg and 570 kBq/µg respectively. Confluent monolayers of HUVEC in 24 well plates were incubated with 100,000 cpm of radiolabeled conjugate in presence of excess of c(RGDfK)-Ata (10 µM), C(RADfK)-Ata (10 µM) and RGD-HSA (0.5 µM) in binding buffer. Cell bound radioactivity was harvested and counted as described above.

Both radiolabeled conjugates were also incubated with confluent C26 carcinoma cells in the absence and presence of an excess of c(RGDfK)-Ata (10 µM). Incubation conditions and analysis of cell-bound radioactivity were as describe above.

Uptake of RGD-equipped Conjugates into Endothelial Cells

HUVEC were incubated with ^{89}Zr-radiolabeled RGDPEG-MMAE-HSA or RGD-MMAE-HSA to determine uptake of the products. The ^{89}Zr-radiolabel will remain trapped inside the cells after degradation of the carrier, in contrast to the ^{125}I-radiolabel. For radiolabeling, 3.7 nmol RGDPEG-MMAE-HSA or RGD-MMAE-HSA was mixed with 18.6 nmol of the chelator TFP-N-succinyldesferal-Fe (desferal) at pH 8.5. After an incubation period of 30 min, the reaction mixture was purified on a Hitrap desalting column (GE Healthcare). UV absorbance at 430 nm was used to assess conjugation of Fe^{3+} containing desferal. Fe^{3+} was replaced with radioactive ^{89}Zr at pH 6.8 as described [17], and the product was purified using a centricon filter unit (MWCO 10 kDa; Millipore, Billerica, MA, USA). Radiochemical purity was 96 % or higher, as determined by trichloroacetic acid precipitation and specific activity was 17.75 MBq/mg and 2.1 MBq/mg for RGDPEG-MMAE-HSA and RGD-MMAE-HSA. Confluent cell layers were incubated with 250,000 cpm ^{89}Zr-RGDPEG-MMAE-HSA or 50,000 cpm ^{89}Zr-RGD-MMAE-HSA at either 4 °C or 37 °C for 4 and 8 hours. Supernatant and cell associated radioactivity were harvested as described above, and radioactivity was counted on a 1282 COMPUGAMMA CS (PerkinElmer, Boston, USA).

In Vitro Killing Efficacy of RGD-equipped Conjugates

HUVEC were plated on 96 well plates (Costar) at 5000 cell/well, and exposed to a graded titration of RGDPEG-MMAE-HSA and RGD-MMAE-HSA. RAD-equipped conjugates were tested at a concentration of 1 and 10 μg/mL. After 72 h of incubation, cell viability was determined by MTS cell viability assay (Promega, Madison, WI, USA) [18]. Absorption was measured on a Thermomax microplate reader (Molecular Devices, Sunnyvale, CA, USA) at 490 nm after 2 h of incubation at 37 °C. Data were analyzed by non-linear regression using GraphPad Prism.

Tumor Accumulation of RGD-equipped Conjugates in Subcutaneous C26 Tumor Model

All animal experiments were performed according to the national law on animal experiments, and were approved by the Animal Ethics Committee of the University of Groningen. Upon arrival, male Balb/C mice were housed in a temperature-controlled room with a 12 h light/dark cycle, and offered ad libitum intake of tap water and standard rodent chow. Mice were anesthetized by Forene (Abbott B.V. Hofddorp, the Netherlands) inhalation in combination with N_2O (600 mL/min) and O_2 (300 mL/min). 1 x 10^6 C26 murine colon carcinoma cells were inoculated subcutaneously in the flank of the mice, and allowed to grow to a size of approximately 8x8 mm. Thereafter a single dose of 30 μg of RGDPEG-MMAE-HSA or RGD-MMAE-HSA was injected in the penis vein under Forene/N_2O/O_2 anesthesia. Mice were sacrificed at 3 h after injection or at 24 h after injection. Tumor, liver, kidney and spleen were collected, and snap frozen in liquid nitrogen.

Immunohistochemical Detection of Conjugates

Cryostat sections (5 μm) prepared from tumor, liver, kidney and spleen were fixed in acetone, and stained for the presence of the conjugates. For this purpose, a rabbit anti-HSA antibody was applied to the sections in a 1:1500 dilution. After removal of endogenous peroxidase activity, staining was

amplified with a peroxidase-conjugated goat anti-rabbit IgG (GARPO, DAKO) followed by a peroxidase-conjugated rabbit anti-goat IgG (RAGPO, DAKO). Peroxidase was visualized by incubation with 3-amino-9-ethyl-carbazole (AEC, Sigma), and sections were counter stained with Mayers hematoxylin (Merck, Darmstadt, Germany) according to standard laboratory protocols.

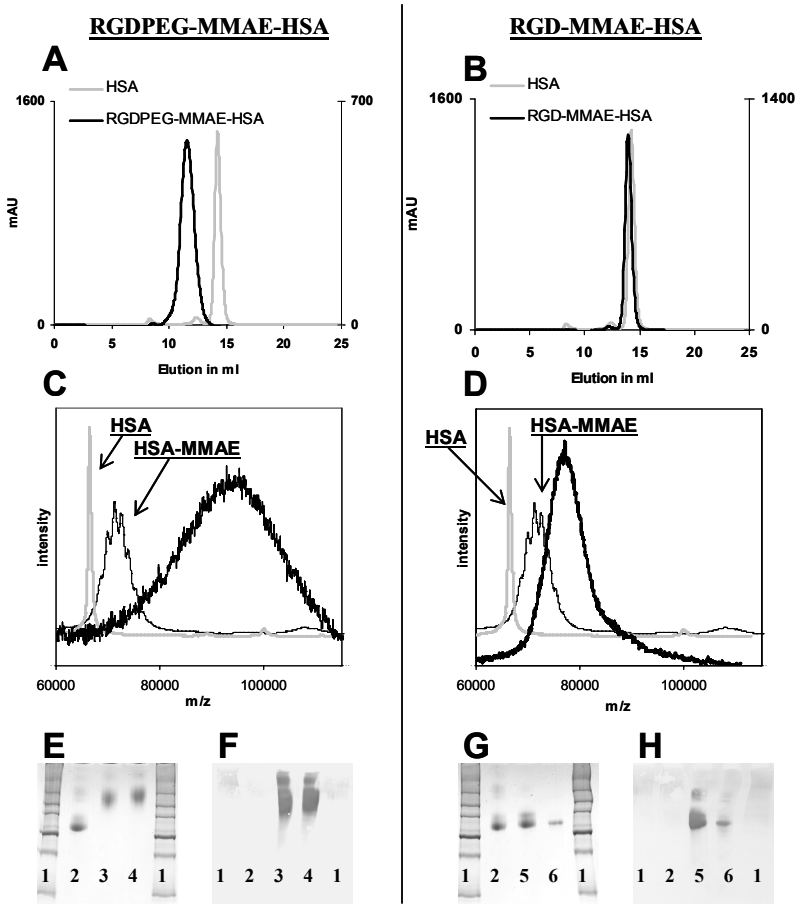

Figure 3.

3A-B: Size exclusion chromatography of RGDPEG-MMAE-HSA(A) and RGD-MMAE-HSA (B) revealed increase in size due to coupling of RGD-peptide via a PEG-linker (A) or a short alkyl linker (B). No aggregates had been formed.

3C-D: MALDI-TOF has been used to estimate molecular weight of RGDPEG-MMAE-HSA (C) and RGD-MMAE-HSA (D). HSA and MMAE-HSA are shown for comparison.

3E-H: SDS-PAGE (E,G) had been performed with a molecular weight marker (1), MMAE-HSA (2), RGDPEG-MMAE-HSA (3), RGDPEG-HSA (4), RGD-MMAE-HSA (5) and RGD-HSA (6). Identical gels have been blotted on a membrane, and were immunostained using anti-RGD antibody (F,H).

Colocalization of conjugates with either tumor endothelium or tumor cells was investigated by fluorescent immunohistochemistry. Deposited conjugate was stained by rabbit anti-HSA antibody

(1:1000 dilution), followed by secondary staining with FITC-conjugated goat anti-rabbit IgG (DAKO). Nuclei were stained using 4'-6-Diamidino-2-phenylindole (DAPI, Sigma). Nuclei of endothelial cells and tumor cells were discriminated by phenotypical differences (endothelial nuclei are flattened, as compared to big tumor cell nuclei).

Results

Synthesis & Characterization

We developed RGD-equipped auristatin conjugates that are directed to $\alpha_v\beta_3$-integrin on angiogenic endothelium (Figure 1). These drug-targeting conjugates were prepared by coupling MMAE and RGD or RGDPEG to an albumin backbone (Figure 2). Both, HPLC and MALDI-TOF analysis demonstrated an average of 4 MMAE per albumin (Table 1, Figure 3). RP-HPLC revealed that the products did not contain free drug or linker molecules. The short SIA linker allowed more RGD to be coupled per HSA compared to the extended PEG linker. Furthermore, RGD numbers were higher in conjugates prepared with parental albumin, not equipped with MMAE (Table 1). SEC analysis demonstrated an increase in size due to the modification, especially for PEGylated products (Figure 3). In addition, it was shown that little aggregation of products occurred, comparable to aggregation found for non-modified HSA. Aggregation hampered further use of drug-targeting conjugates only when drug loads of eight MMAE per albumin were tested (data not shown). Coupling of RGD-peptide onto the distal end of PEG was demonstrated by anti-RGD western blot. Both products as well as their respective control products RGDPEG-HSA and RGD-HSA were positively stained by anti-RGD antibody, while MMAE-HSA was not stained (Figure 3).

Table 1. Characterization of drug-targeting conjugates by MALDI-TOF

	number of modifications per HSA		MW in kDa
	MMAE	RGDPEG or RGD	
RGDPEG-MMAE-HSA	4.1	5.4	94.5
RGDPEG-HSA	-	7.1	96.1
RGD-MMAE-HSA	4.1	7.6	77.3
RGD-HSA	-	13.2	76.2

Binding Specificity of RGD-equipped Conjugates to Endothelial Cells and C26 Carcinoma Cells

Binding specificity was evaluated using ^{125}I-labelled drug-targeting conjugates. Both conjugates bound to $\alpha_v\beta_3$-integrin expressing HUVEC, and could be completely displaced by excess of RGD-peptide or RGD-HSA but not by RAD-peptide (Figure 4A). This demonstrated that binding was mediated exclusively by the introduced RGD-moiety. Remarkably, a 4 times higher binding of ^{125}I-RGD-MMAE-HSA than of ^{125}I-RGDPEG-MMAE-HSA was observed. Both conjugates bound also to C26 cells but in contrast to HUVEC no difference in the quantity of binding could be detected.

Binding to C26 cells was as well mediated by the introduced RGD-moiety, as could be concluded from the complete displacement by RGD-peptide (Figure 4B).

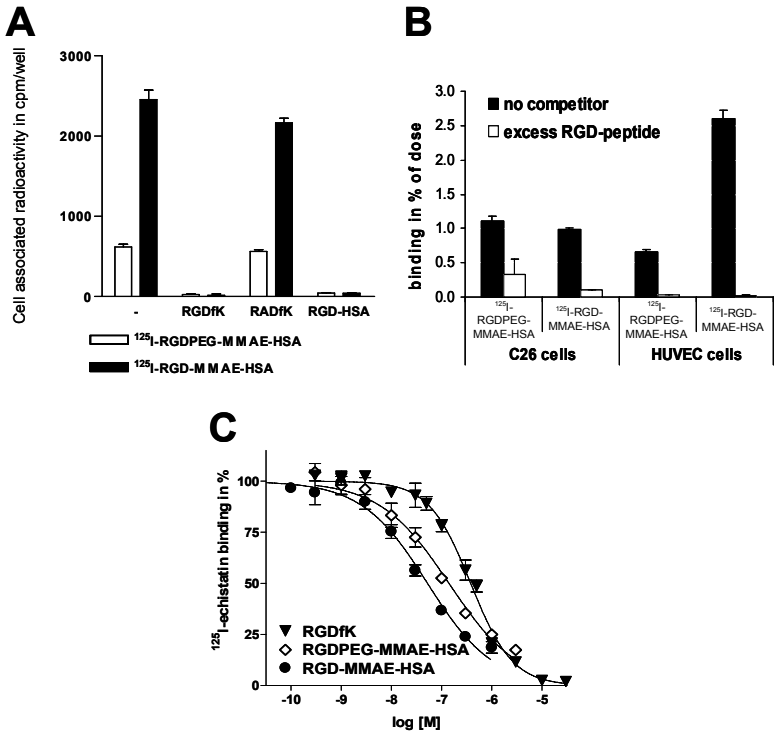

Figure 4. Binding properties of drug targeting conjugates.

(A) Binding specificity was tested by coincubation of radiolabeled drug-targeting conjugates with excess of c(RGDfK)-Ata (10 µM), c(RADfK)-Ata (10 µM) and RGD-HSA (0.3 µM) on $\alpha_v\beta_3$-expressing HUVEC.

(B) Radiolabeled drug-targeting conjugates were incubated with C26 carcinoma cells and HUVEC. Specificity of binding was determined by conincubation with excess of c(RGDfK)-Ata (10 µM).

(C) Binding affinity is detected by competition between ^{125}I-echistatin, and increasing concentrations of drug-targeting conjugates for $\alpha_v\beta_3$-integrin on HUVEC. Concentrations are expressed in mol/l.

Binding Affinity of RGD-equipped Conjugates to Endothelial Cells

Binding affinity of drug-targeting conjugates was determined in competition experiments with the known $\alpha_v\beta_3$-integrin ligand ^{125}I-echistatin as shown in Figure 4C. Both conjugates displaced ^{125}I-echistatin in the low nanomolar range, with the binding affinity of RGD-MMAE-HSA being higher than of RGDPEG-MMAE-HSA. The respective control conjugate RGDPEG-HSA and RGD-HSA displayed higher affinities (Table 2). All conjugates possessed an increased affinity for $\alpha_v\beta_3$-integrin as compared to the single c(RGDfK) peptide. Furthermore, a clear relationship was observed between the average number of RGD/albumin and affinity for the target cells. The observation that multivalent RGD-carriers bind with higher affinity than monovalent carriers has been made before [12, 19, 20].

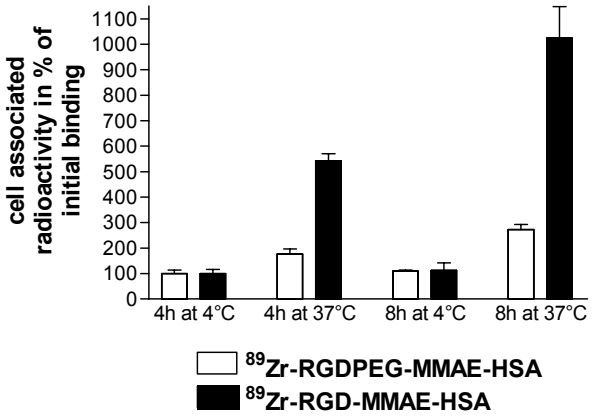

Figure 5. ^{89}Zr-RGDPEG-MMAE-HSA and ^{89}Zr-RGD-MMAE-HSA were incubated with HUVEC at 4 and 37 °C for 4 or 8 h to determine uptake of the drug-targeting conjugates.

Uptake of RGD-equipped Conjugates into Endothelial Cells

Drug-targeting conjugates were labeled with ^{89}Zr to study intracellular uptake. ^{89}Zr, captured by the chelator desferal, is highly stable, and its hydrophilicity will lead to its entrapment inside the cells after degradation of the carrier [21, 22]. As such it is an ideal label for uptake studies since this will prevent redistribution of the radiolabel. In spite of all previous modifications we were able to attach 1.2 (RGDPEG-MMAE-HSA) and 0.9 (RGD-MMAE-HSA) desferal per conjugate. ^{89}Zr labeled conjugates were incubated with HUVEC at 4 °C and 37 °C degrees. Energy dependent uptake processes take place at 37 °C, at which more cell associated radioactivity was found than at 4 °C (Figure 5), at which these processes are inhibited. The cell associated radioactivity increased further upon longer incubation at 37 °C but not at 4 °C. Taken together, these results indicated uptake of the drug-targeting conjugates via an active process. Uptake was more pronounced for ^{89}Zr-RGD-MMAE-HSA than for ^{89}Zr-RGDPEG-MMAE-HSA (black versus white bars).

In Vitro Killing Efficacy of RGD-equipped Conjugates

Monomethyl auristatin E has been shown to inhibit the polymerization of tubulin in dividing cells, and thus to induce apoptosis [3]. To study the effect of intracellularly delivered MMAE, HUVEC were exposed for 72 h to serial dilutions of both drug-targeting conjugates and their respective control. Regression analysis of the concentration-cytotoxicity curves in Figure 6A revealed EC_{50}s (effective concentrations) of 44 nM for RGDPEG-MMAE-HSA and 6.6 nM for RGD-MMAE-HSA. In contrast, the RAD-containing control conjugates and the control conjugates without MMAE showed no effect at concentration as high as 150 nM (Figure 6B).

Preliminary In Vivo Evaluation

To determine whether the RGD-equipped drug carriers accumulate in the tumor endothelium, we administered RGDPEG-MMAE-HSA and RGD-MMAE-HSA to C26 murine colon carcinoma bearing mice. Anti-HSA staining of sections of organs and tumors showed the presence of both

conjugates in the tumor, three hours after injection (Figure 7A,F). In contrast, hardly any drug-targeting conjugate was found in the spleen and kidneys. A clear staining was detected in the liver. Higher magnification revealed the presence of the drug-targeting conjugates in the hepatic sinusoids, not confined to any sinusoidal cell type.

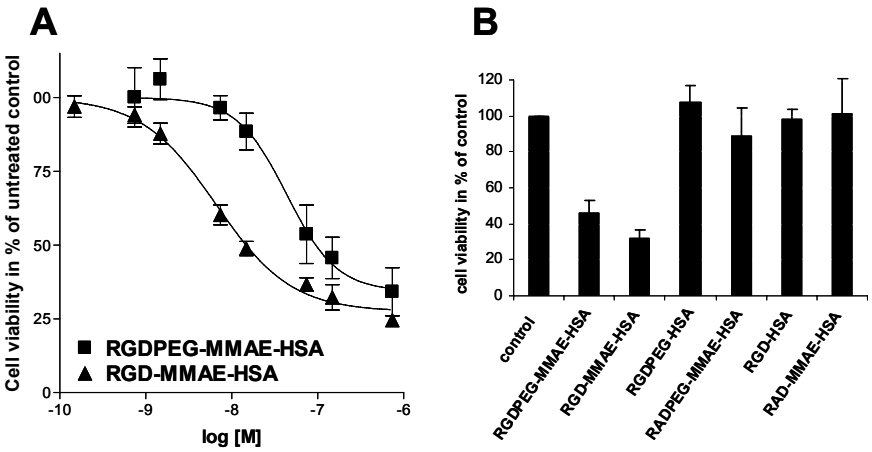

Figure 6. (A) HUVEC have been incubated with increasing concentrations of drug-targeting conjugates to determine killing efficacy. Concentrations are expressed in mol/l. (EC_{50}s: RGDPEG-MMAE-HSA 41 nM; RGD-MMAE-HSA 6.6 nM). (B) Viability of HUVEC treated with 150 nM of drug targeting and control conjugates.

Table 2. Binding and cell killing potency of drug-targeting conjugates

	RGD-peptides per HSA	EC_{50} in nM	Binding	
			IC_{50} in nM	Fold increase vs RGD
RGDPEG-MMAE-HSA	5.4	41.1	141	2.7
RADPEG-MMAE-HSA		> 150[a]	> 1000[a]	-
RGDPEG-HSA	7.1		18.6	21
RGD-MMAE-HSA	7.6	6.64	52.6	7.3
RAD-MMAE-HSA		> 150[a]	> 300[a]	-
RGD-HSA	13.2		5.90	65
c(RGDfK)-Ata			382	1

[a] highest tested concentration.

This distribution pattern changed after 24 h. RGD-MMAE-HSA could not be detected in any of the three control organs (Figure 7H-J) while a clear accumulation in the tumor could be detected (Figure 7G). RGDPEG-MMAE-HSA was also absent in kidneys and spleen but showed some

residual staining in the liver (Figure 7C-E), apart from the pronounced tumor accumulation (Figure 7B).

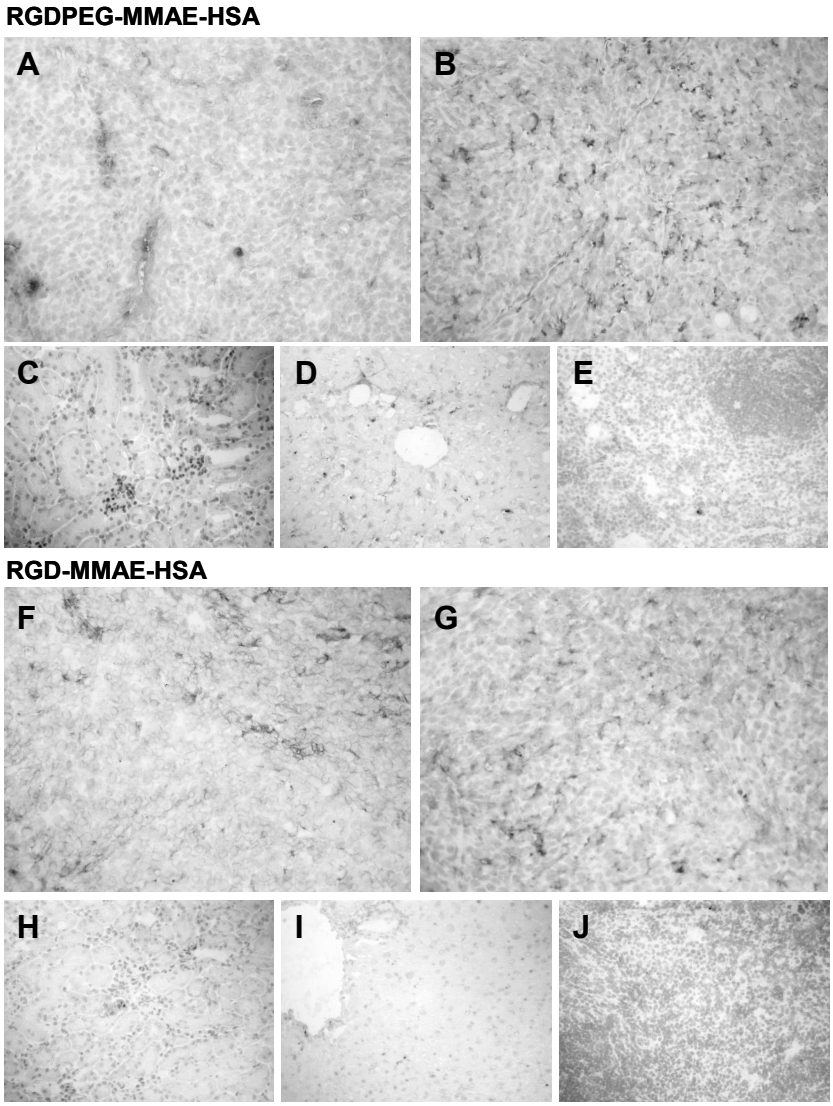

Figure 7. C26 tumor bearing mice had been injected with either 30 µg RGDPEG-MMAE-HSA (A-E) or RGD-MMAE-HSA (F-J). Sections were stained with rabbit antiHSA antibody. Both drug-targeting conjugates localized in C26 tumors 3 h (A,F) and 24 h (B,G) after i.v. administration. Sections of kidney (C,H), liver (I) and spleen (E,J) at 24 h time point are stained negative. All pictures are taken at magnification of 200x; C-E and H-J are reduced to 45% of the size of A, B, F and G. The color picture can be found in the appendix.

To identify which cell types had accumulated the auristatin-albumin conjugates, we investigated the colocalization of the albumins with either endothelial cells or tumor cells. Since endothelial cells display typically flattened nuclei in contrast to bigger nuclei for C26 cells, DAPI nuclear staining could be used to discriminate between vasculature and tumor cells. Figure 8 shows the typical fluorescent staining for cell nuclei (blue) and HSA (green) of a tumor 24 h after injection of RGD-MMAE-HSA (Figure 8A) and RGDPEG-MMAE-HSA (Figure 8B). A blood vessel with two typically flattened endothelial nuclei is pointed out by red arrows, while some of the larger tumor cell nuclei are indicated by yellow arrows. HSA was found along the vessel wall, but also colocalized with tumor cells within the tumor mass.

Discussion

Immunotoxins are an attractive strategy to kill specific cell types without affecting other cells in the body. Typically, such conjugates have been prepared by conjugating cytotoxic agents to antibodies [23]. We now report on a different type of target-cell specific toxin containing conjugate, in which RGD-peptides facilitate recognition of angiogenic endothelial cells (Figure 1). The RGD-motif is a highly conserved receptor binding ligand, and allows studying RGD-equipped drug targeting in different species without further modification of the homing ligand. This is not possible for antibodies that commonly are species specific. RGD-equipped albumin conjugates are a versatile platform that can be readily modified with drugs, and tailored with other moieties such as PEG. HSA functions in this context as a monomeric polymer featuring low immunogenicity, high biocompatibility and excellent biodegradability. Furthermore, renal filtration of drug is prevented by the high molecular size of albumin enabling prolonged exposure of the target cells to the conjugates. Here we report the development of RGD-MMAE-HSA and RGDPEG-MMAE-HSA, in which MMAE-HSA is equipped with RGD-peptide via a short alkyl linker or via an extended PEG linker (Figure 2). MALDI-TOF analysis of synthesis products demonstrated that both conjugates were modified with multiple RGD-peptides. It has been recognized that RGD-based drug-targeting conjugates need to be equipped with multiple RGD-peptides in order to obtain optimal binding to and uptake into the target cell [11, 24] and current research focuses on various multivalent carriers for delivery of therapeutic or diagnostic agents [25-29]. The presently developed drug-targeting conjugates both demonstrated multivalent binding, as they bind with higher affinity than single RGD-peptide, and they are also taken up, thus fulfilling these criteria. However, application of the short alkyl linker resulted in a higher average RGD/carrier ratio than the PEG linker. As a consequence RGD-MMAE-HSA bound with higher affinity and in higher quantity to $\alpha_v\beta_3$-expressing HUVEC than RGDPEG-MMAE-HSA. We did not fractionate our products further into batches with a narrow RGD/HSA ratio, and it can be conceived that individual RGDPEG-MMAE-HSA with high RGD loading will bind stronger to the target cells. Another explanation for the difference in affinity might be a different spatial presentation of RGD-peptides due to the extended PEG linker, or differences in hydrophobicity between the two linkers.

In line with the observed higher affinity and higher uptake efficiency, RGD-MMAE-HSA demonstrated superior EC_{50} in cell killing as compared to the PEGylated conjugates. This result was corroborated upon testing of RGD-MMAE-HSA bearing an average of six MMAE molecules but less RGD-peptides per carrier, since only little improvement in EC_{50} was found (data not shown). Taken

together, these data indicate that a high number of RGD-peptides and efficient internalization is more important than a high drug load.

Both drug-targeting conjugates demonstrated efficient killing of the target cells at nanomolar concentrations. The EC_{50} values (Table 2) are in a similar range as EC_{50} values of MMAE modified antibodies against E-selectin [6], CD20 on non-Hodgkin's lymphoma [4], TMEFF2, a plasma membrane protein overexpressed in prostate cancer [5], and the glycoprotein NMB found on melanoma [30]. In vitro cell killing assays showed that a fraction of the cells survived treatment with highest concentrations of immunoconjugates [5, 6, 31]. Identical observations were made for our RGD-based conjugates. Most likely, this fraction represented not dividing cells, which therefore do not respond to MMAE.

The short alkyl linker was chosen to modify MMAE-HSA with a maximum of RGD-peptides but the extended PEG linker was chosen for its known ability to shield the modified HSA, to prolong circulation time, and to increase passive targeting by the enhanced permeability and retention (EPR) effect [32, 33]. These advantages can not be detected in in vitro assays. In the C26 tumor bearing mice, both conjugates accumulated to a similar extent in the tumors in time, with a stronger and more widespread localization for the conjugates after 24 h compared to localization at 3 h. At the later time point, kidney, liver and spleen were almost devoid of drug-targeting conjugates. Thus, the concentration of drug-targeting conjugate increased in the tumor, and at the same time the concentration in organs decreased. Mitra et al [34], reported similar findings, in which a RGD-equipped polymer accumulated in the course of three days in prostate tumors.

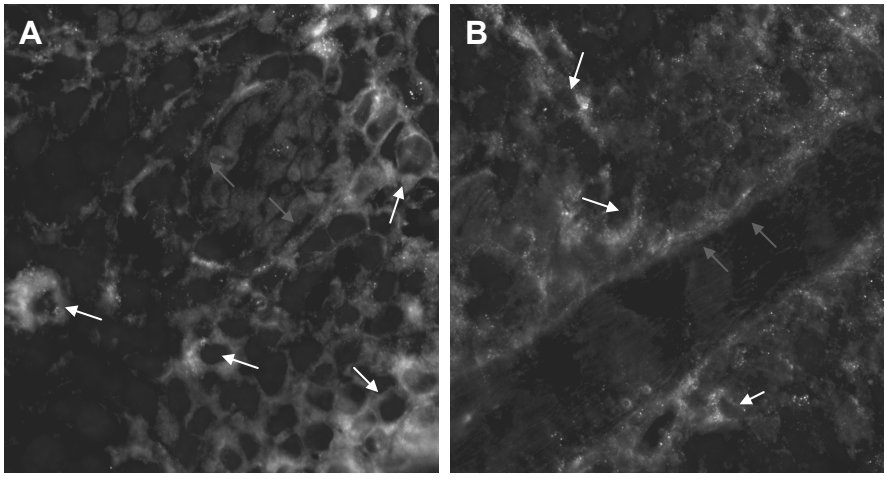

Figure 8. Colocalization of auristatin-albumin conjugates with tumor vasculature and tumor cells. C26 tumor section of RGDPEG-MMAE-HSA (8A) and RGD-MMAE-HSA (8B) treated mice (24h post injection) were stained with DAPI (blue) to visualize endothelial cells (flattened nuclei) or tumor cells (big nuclei). Accumulated conjugate was visualized by anti-HSA staining (green). Red arrows point at the typically flattened nuclei of endothelial cells and identify a blood vessel, colocalizing with HSA. Examples for tumor cells nuclei that colocalize with HSA are pointed out using yellow arrows. Magnification 400x. Color picture can be found in the appendix.

RGDPEG-MMAE-HSA was still detectable in the liver 24h after injection. A possible explanation for this might be a longer circulation time and delayed degradation compared to RGD-MMAE-HSA due to the PEG moiety. A remarkably strong staining at both time points and for both conjugates was observed in tumor tissue. It is important to note that not a tracer dose but a therapeutic dose (30 µg/mouse) was given, thus reflecting the distribution pattern during treatment. In the future experiments, we will use the here prepared ^{89}Zr-labeled conjugates in combination with positron emission tomography (PET) to gain more insight in organ distribution of RGD-equipped drug-albumin conjugates. In those studies, tumor accumulation of RGD-based carriers will also be compared to carriers that accumulate in tumors by EPR, such as for instance the above presented RAD-modified albumins. ^{89}Zirkonium captured by the chelator desferal is the ideal label for these studies as it is highly stable, hydrophilic enough to prevent redistribution, and equipped with a half-life that allows PET scans for longer than 48h.

The preliminary distribution data of our product indicated that the accumulation in the tumor was widespread, and did not reflect a vascular staining pattern. Fluorescent staining of nuclei demonstrated colocalization of the conjugates with both endothelial cells and tumor cells. We therefore investigated binding of ^{125}I-labeled conjugates to C26 tumor cells. Indeed, both RGDPEG-MMAE-HSA and RGD-MMAE-HSA bound to C26 cells, and were displaceable by coincubation with an excess of free RGD-peptide. This indicated that binding was mediated via the RGD-peptide to C26 carcinoma cells, and binding presumable took place via $\alpha_v\beta_3$-integrin or related α_v integrins. Thus angiogenic endothelium and tumor cells were both targeted in the chosen tumor model, explaining the staining pattern. An $\alpha_v\beta_3$-integrin expressing tumor is likely to be more responsive than a $\alpha_v\beta_3$-integrin negative tumor. Although this may perturbate the selectivity of the RGD-equipped conjugates for the tumor vasculature per se, this will even enhance the potential antitumor effects of the compounds. Similarly, many of the studies employing RGD-peptides for either imaging or drug delivery have been conducted in tumor models that express $\alpha_v\beta_3$-integrin at the tumor cells [11].

In conclusion, two types of RGD-equipped auristatin-albumin conjugates have been developed, demonstrating the versatility of such a targeting approach. Both drug-targeting conjugates displayed excellent binding and cell killing properties, and strongly accumulate in a C26 tumor in mice. These results indicate that RGD-mediated targeting of auristatin E is a promising strategy for delivery of a proapoptotic payload to tumor vasculature and carcinoma cells, and a valid alternative to current immunoconjugates. In the future pharmacokinetics and tumor growth inhibition of these promising compounds will be evaluated in detail.

Acknowledgment

J. H. Pol from the Department of Nuclear Medicine is kindly acknowledged for radiolabeling of proteins, H. E. Moorlag from the Endothelial Cell Facility UMCG for skillful isolation and culturing of HUVEC, and Annemiek van Loenen-Weemaes for assistance with animal experiments. We also acknowledge Prof. G. A. M. S. van Dongen and Ir. L. R. Perk of the VU medical center for providing the desferal labeling technology. This work was made possible by grants from Marie Curie (HPMI-CT-2002-00218) and SenterNovem (TSGE1083).

Reference List

(1) Ferrara N, Kerbel RS. Angiogenesis as a therapeutic target. Nature 2005 Dec 15;438(7070):967-974.
(2) Pettit GR. The dolastatins. Fortschr Chem Org Naturst 1997;70:1-79.
(3) Doronina SO, Toki BE, Torgov MY, Mendelsohn BA, Cerveny CG, Chace DF, et al. Development of potent monoclonal antibody auristatin conjugates for cancer therapy. Nat Biotechnol 2003 Jul;21(7):778-784.
(4) Law CL, Cerveny CG, Gordon KA, Klussman K, Mixan BJ, Chace DF, et al. Efficient elimination of B-lineage lymphomas by anti-CD20-auristatin conjugates. Clin Cancer Res 2004 Dec 1;10(23):7842-7851.
(5) Afar DE, Bhaskar V, Ibsen E, Breinberg D, Henshall SM, Kench JG, et al. Preclinical validation of anti-TMEFF2-auristatin E-conjugated antibodies in the treatment of prostate cancer. Mol Cancer Ther 2004 Aug;3(8):921-932.
(6) Bhaskar V, Law DA, Ibsen E, Breinberg D, Cass KM, DuBridge RB, et al. E-selectin up-regulation allows for targeted drug delivery in prostate cancer. Cancer Res 2003 Oct 1;63(19):6387-6394.
(7) Sanderson RJ, Hering MA, James SF, Sun MM, Doronina SO, Siadak AW, et al. In vivo drug-linker stability of an anti-CD30 dipeptide-linked auristatin immunoconjugate. Clin Cancer Res 2005 Jan 15;11(2 Pt 1):843-852.
(8) Dubowchik GM, Mosure K, Knipe JO, Firestone RA. Cathepsin B-sensitive dipeptide prodrugs. 2. Models of anticancer drugs paclitaxel (Taxol), mitomycin C and doxorubicin. Bioorg Med Chem Lett 1998 Dec 1;8(23):3347-3352.
(9) Dubowchik GM, Firestone RA, Padilla L, Willner D, Hofstead SJ, Mosure K, et al. Cathepsin B-labile dipeptide linkers for lysosomal release of doxorubicin from internalizing immunoconjugates: model studies of enzymatic drug release and antigen-specific in vitro anticancer activity. Bioconjug Chem 2002 Jul;13(4):855-869.
(10) Pierschbacher MD, Ruoslahti E. Cell attachment activity of fibronectin can be duplicated by small synthetic fragments of the molecule. Nature 1984 May 3;309(5963):30-33.
(11) Temming K, Schiffelers RM, Molema G, Kok RJ. RGD-based strategies for selective delivery of therapeutics and imaging agents to the tumour vasculature. Drug Resist Updat 2005 Dec;8(6):381-402.
(12) Kok RJ, Schraa AJ, Bos EJ, Moorlag HE, Asgeirsdottir SA, Everts M, et al. Preparation and functional evaluation of RGD-modified proteins as alpha(v)beta(3) integrin directed therapeutics. Bioconjug Chem 2002 Jan;13(1):128-135.
(13) Schraa AJ, Kok RJ, Berendsen AD, Moorlag HE, Bos EJ, Meijer DK, et al. Endothelial cells internalize and degrade RGD-modified proteins developed for tumor vasculature targeting. J Control Release 2002 Oct 4;83(2):241-251.
(14) Schraa AJ, Kok RJ, Botter SM, Withoff S, Meijer DK, de Leij LF, et al. RGD-modified anti-CD3 antibodies redirect cytolytic capacity of cytotoxic T lymphocytes toward alphavbeta3-expressing endothelial cells. Int J Cancer 2004 Nov 1;112(2):279-285.
(15) Kumar CC, Nie H, Rogers CP, Malkowski M, Maxwell E, Catino JJ, et al. Biochemical characterization of the binding of echistatin to integrin alphavbeta3 receptor. J Pharmacol Exp Ther 1997 Nov;283(2):843-853.
(16) HUNTER WM, GREENWOOD FC. Preparation of iodine-131 labelled human growth hormone of high specific activity. Nature 1962 May 5;194:495-496.
(17) Verel I, Visser GW, Boellaard R, Stigter-van WM, Snow GB, van Dongen GA. 89Zr immuno-PET: comprehensive procedures for the production of 89Zr-labeled monoclonal antibodies. J Nucl Med 2003 Aug;44(8):1271-1281.
(18) Alley MC, Scudiero DA, Monks A, Hursey ML, Czerwinski MJ, Fine DL, et al. Feasibility of drug screening with panels of human tumor cell lines using a microculture tetrazolium assay. Cancer Res 1988 Feb 1;48(3):589-601.
(19) Schraa AJ, Kok RJ, Moorlag HE, Bos EJ, Proost JH, Meijer DK, et al. Targeting of RGD-modified proteins to tumor vasculature: a pharmacokinetic and cellular distribution study. Int J Cancer 2002 Dec 10;102(5):469-475.
(20) Thumshirn G, Hersel U, Goodman SL, Kessler H. Multimeric cyclic RGD peptides as potential tools for tumor targeting: solid-phase peptide synthesis and chemoselective oxime ligation. Chemistry 2003 Jun 16;9(12):2717-2725.
(21) Verel I, Visser GW, Boerman OC, van Eerd JE, Finn R, Boellaard R, et al. Long-lived positron emitters zirconium-89 and iodine-124 for scouting of therapeutic radioimmunoconjugates with PET. Cancer Biother Radiopharm 2003 Aug;18(4):655-661.
(22) Perk LR, Visser GW, Vosjan MJ, Stigter-van WM, Tijink BM, Leemans CR, et al. (89)Zr as a PET surrogate radioisotope for scouting biodistribution of the therapeutic radiometals (90)Y and (177)Lu in tumor-bearing nude mice after coupling to the internalizing antibody cetuximab. J Nucl Med 2005 Nov;46(11):1898-1906.
(23) Wu AM, Senter PD. Arming antibodies: prospects and challenges for immunoconjugates. Nat Biotechnol 2005 Sep;23(9):1137-1146.
(24) Wester HJ, Kessler H. Molecular targeting with peptides or peptide-polymer conjugates: just a question of size? J Nucl Med 2005 Dec;46(12):1940-1945.
(25) Temming K, Lacombe M, Schaapveld RQJ, Orfi L, Keri G, Poelstra K, et al. Rational Design of RGD-albumin conjugates for targeted delivery of the VEGF-R kinase inhibitor PTK787 to angiogenic endothelium. ChemMedChem 2006;11:1200-1203.
(26) Temming K, Lacombe M, van der Hoeven P, Prakash J, Gonzalo T, Dijkers ECF, et al. Delivery of the p38 MAPkinase inhibitor SB202190 to angiogenic endothelial cells: development of novel RGD-equipped and pegylated drug-albumin conjugates using platinum(II) based drug linker technology. Bioconjug Chem 2006 Sep 20;17(5):1246-1255.
(27) Toublan FJ, Boppart S, Suslick KS. Tumor targeting by surface-modified protein microspheres. J Am Chem Soc 2006 Mar 22;128(11):3472-3473.
(28) Kim WJ, Yockman JW, Jeong JH, Christensen LV, Lee M, Kim YH, et al. Anti-angiogenic inhibition of tumor growth by systemic delivery of PEI-g-PEG-RGD/pCMV-sFlt-1 complexes in tumor-bearing mice. J Control Release 2006 Sep 12;114(3):381-388.

(29) Shukla R, Thomas TP, Peters J, Kotlyar A, Myc A, Baker J, Jr. Tumor angiogenic vasculature targeting with PAMAM dendrimer-RGD conjugates. Chem Commun (Camb) 2005 Dec 14;(46):5739-5741.
(30) Tse KF, Jeffers M, Pollack VA, McCabe DA, Shadish ML, Khramtsov NV, et al. CR011, a fully human monoclonal antibody-auristatin E conjugate, for the treatment of melanoma. Clin Cancer Res 2006 Feb 15;12(4):1373-1382.
(31) Francisco JA, Cerveny CG, Meyer DL, Mixan BJ, Klussman K, Chace DF, et al. cAC10-vcMMAE, an anti-CD30-monomethyl auristatin E conjugate with potent and selective antitumor activity. Blood 2003 Aug 15;102(4):1458-1465.
(32) Tanaka T, Shiramoto S, Miyashita M, Fujishima Y, Kaneo Y. Tumor targeting based on the effect of enhanced permeability and retention (EPR) and the mechanism of receptor-mediated endocytosis (RME). Int J Pharm 2004 Jun 11;277(1-2):39-61.
(33) Caliceti P, Veronese FM. Pharmacokinetic and biodistribution properties of poly(ethylene glycol)-protein conjugates. Adv Drug Deliv Rev 2003 Sep 26;55(10):1261-1277.
(34) Mitra A, Mulholland J, Nan A, McNeill E, Ghandehari H, Line BR. Targeting tumor angiogenic vasculature using polymer-RGD conjugates. J Control Release 2005 Jan 20;102(1):191-201.